Journal of ELECTRONIC MATERIALS, Vol. 41, No. 11, 2012
DOI: 10.1007/s11664-012-2202-7

Electrodeposition of Sb_xTe_y Thermoelectric Films from Dimethyl Sulfoxide Solution

FEI-HUI LI,[1] WEI WANG,[2,4] YUN-LAN GONG,[1] and JIAN-YING LI[3]

1.—Department of Applied Chemistry, School of Science, Tianjin University of Commerce, Tianjin 300134, People's Republic of China. 2.—Department of Applied Chemistry, School of Chemical Engineering and Technology, Tianjin University, Tianjin 300072, People's Republic of China. 3.—Tianjin Xuanzhen Bio-medicine and Science Development Co., Ltd., Tianjin 300457, People's Republic of China. 4.—e-mail: wwtju@yahoo.cn

The electrochemical behaviors of nonaqueous dimethyl sulfoxide solutions containing Te^{IV} and Sb^{III} were investigated using cyclic voltammetry. On this basis, Sb_xTe_y thermoelectric films were prepared by the potentiodynamic electrodeposition technique from nonaqueous dimethyl sulfoxide solution, and the composition, morphology, and thermoelectric properties of the films were analyzed. Sb_xTe_y thermoelectric films prepared under different potential ranges all possessed smooth morphology. After annealing treatment at 200°C under N_2 protection for 4 h, all the deposited films showed *p*-type semiconductor properties. $Sb_{1.87}Te_{3.13}$ thermoelectric film, which most closely approached the stoichiometry of Sb_2Te_3 and possessed the highest Seebeck coefficient, could be potentiodynamically electrodeposited in the potential range of −200 mV to −600 mV.

Key words: Electrodeposition, DMSO, Sb_xTe_y films, performance

INTRODUCTION

Thermoelectric materials and cells have attracted considerable interest due to the requirement for environmental protection and military applications. Bismuth and antimony telluride-based materials are considered to be the best materials for use in thermoelectric devices in the temperature range of 200 K to 400 K. Electrodeposition of bismuth telluride, bismuth antimony telluride, and bismuth selenium telluride and analysis of the electrochemical behaviors of the corresponding ions in aqueous solutions has been a topic of recent experimental research.[1–9] This technique presents a convenient and inexpensive method for fabricating thermoelectric microdevices. The most advantageous point of the technique is that the doping concentration and crystalline state of the thermoelectric films can be easily controlled by adjusting the electrodeposition parameters.[10] However, there is great difficulty in fabricating Sb_xTe_y film materials with compact structure and smooth surface from aqueous solutions, since the electrodeposition potentials of Te^{IV} and Sb^{III} are far from each other in aqueous systems. Considering that the reduction potentials of ions in nonaqueous systems may be very different from those in aqueous systems, some researches started to focus on the co-electrodeposition process of Bi^{III} and Te^{IV} from nonaqueous systems[11–14] (such as organic systems and molten salt systems), but related research does not provide many results on the electrodeposition mechanism and properties of such deposits prepared in nonaqueous systems.

In our laboratory, nonaqueous dimethyl sulfoxide (DMSO) was chosen as the solvent of the nonaqueous system, since it possesses strong polarity, a wide electrochemical window, and high stability. The electrochemical behaviors of DMSO solutions containing Te^{IV} and Sb^{III} were firstly investigated by electrochemical methods. Then, Sb_xTe_y films were prepared from DMSO solution, and the effects of electrodeposition parameters as well as the annealing treatment were examined. Performance characterizations were also conducted.

(Received March 29, 2012; accepted July 10, 2012; published online August 10, 2012)

EXPERIMENTAL PROCEDURES

Solution

Te^{IV} solution was prepared by dissolution of $TeCl_4$ (analytical reagent) in nonaqueous DMSO solution. Sb^{III} solution was obtained in the same way, by dissolution of $SbCl_3$ (analytical reagent). Sb-Te mixed solution was obtained by mixing the above solutions firstly and then adding with 0.1 M KNO_3 as the supporting electrolyte. The concentrations of the different solutions are detailed in Table I.

Electrochemical Measurements

All electrochemical measurements were performed using a CHI660B electrochemical working station at 25 ± 1°C. A standard three-electrode cell was used for the electrochemical measurements, consisting of an Au plate (1 cm^2) as the working electrode, a Pt plate as the auxiliary electrode, and a saturated calomel electrode (SCE) as the reference electrode. The working electrode was mechanically polished, electrochemically degreased, etched in concentrated HNO_3 solution, rinsed with redistilled water and absolute ethyl alcohol, and dried with cold air to ensure a clean surface before measurements. All potentials were measured and are expressed relative to SCE. A magnetic stirrer was used to stir the electrolyte when needed. The substrates used for the electrodeposition of Sb_xTe_y film were copper sheets covered with a layer of electrodeposited gold film (about 600 nm). The electrodeposition time was adjusted to maintain a total passed electric charge of 10 C/cm^2, and the average thickness was about 4 μm.

Cyclic voltammograms (CV) and linear sweep voltammograms (LSV) were recorded at scanning rates of 10 mV/s and 0.1 mV/s, respectively, and all the CV presented herein are for the first recorded cycle.

Characterization of the Electrodeposited Films

The x-ray diffraction (XRD) patterns of the films were obtained with a film x-ray diffractometer using Cu K_α radiation (Philips PANalytical X'pert MPD, 40 kV, 200 mA, scan rate 4°/min). The film composition was detected using an energy-dispersive spectrometer (EDS, OXFORD ISIS300). The Seebeck coefficient and resistance of the prepared thermoelectric films were measured using an EC2001 Seebeck coefficient measurement system developed by Tianjin University and a Keithley 2000 multimeter (manufactured by Keithley Instruments Inc.) at 25 ± 1°C, respectively. The Seebeck coefficient measurements were conducted along the thickness direction of the films (parallel to the growth direction of the electrodeposited film), and the applied thermal difference was controlled to 10°C. The resistance measurements were conducted along the same direction.

Table I. Concentrations of different solutions

Solution	$TeCl_4$	$SbCl_3$	KNO_3
Te^{IV} solution	20 mM	–	–
Sb^{III} solution	–	20 mM	–
Sb-Te binary solution	20 mM	20 mM	0.1 M

RESULTS AND DISCUSSION

Electrochemical Behaviors of Individual Te^{IV} and Sb^{III} Solution Systems

The electrochemical behaviors of individual Te^{IV} and Sb^{III} solution systems were examined by cyclic voltammetry, and the results are shown in Fig. 1. It can be seen that only a couple of reduction/oxidation peaks located at −0.87 V/0.56 V can be observed in Fig. 1a, corresponding to the reduction/oxidation process of Te^{IV}/Te^0. For the reduction/oxidation process of Sb^{III}/Sb^0, two reduction peaks and one oxidation peak can be found in Fig. 1b. This reveals that the reduction process of Sb^{III} is more complicated than that of Te^{IV}, and the formation of Sb^0 during the cathodic process is completed through a multistep process. No obvious deposit can be observed during the cathodic scanning process until the cathodic scanning potential shifts into the potential range of peak A and peak D in Fig. 1a and b, respectively. The identity of the deposit obtained in these potential ranges in the corresponding solution system was determined to be elemental Te^0 and Sb^0 by XRD analyses. The obvious differences in the peak potentials and peak shapes between the reduction peaks and oxidization peaks reveal that the reduction/oxidation of Te^{IV} and Sb^{III} in DMSO solutions are all irreversible processes on Au electrode. In addition, comparing the cathodic process of curve (a) and curve (b), it can be found that, during the cathodic scanning process, the current density of curve (a) starts to increase at more positive potential. These results indicate that the reduction process of Te^{IV} is much easier than that of Sb^{III}.

Figure 2 shows the LSV measured in DMSO solutions containing 20 mM Te^{IV} and 20 mM Sb^{III}, respectively. It can be seen that reduction of Te^{IV} begins at −50 mV; its cathodic current density increases slowly as the potential becomes more negative, and the concentration polarization is not the rate-controlling step until the cathodic polarization potential reaches −260 mV. For the LSV curve of Sb^{III}, two plateaus, corresponding to the two reduction peaks in the cathodic branch of the CV curve obtained in Sb^{III} solution (Fig. 1a), can be observed. These results further confirm that reduction of Sb^{III} in DMSO solution is completed through multiple steps. Comparing the heights of the two plateaus in the LSV curve of Sb^{III} and the areas of the two reduction peaks in the cathodic branch of the CV curve of Sb^{III}, it can be considered that reduction

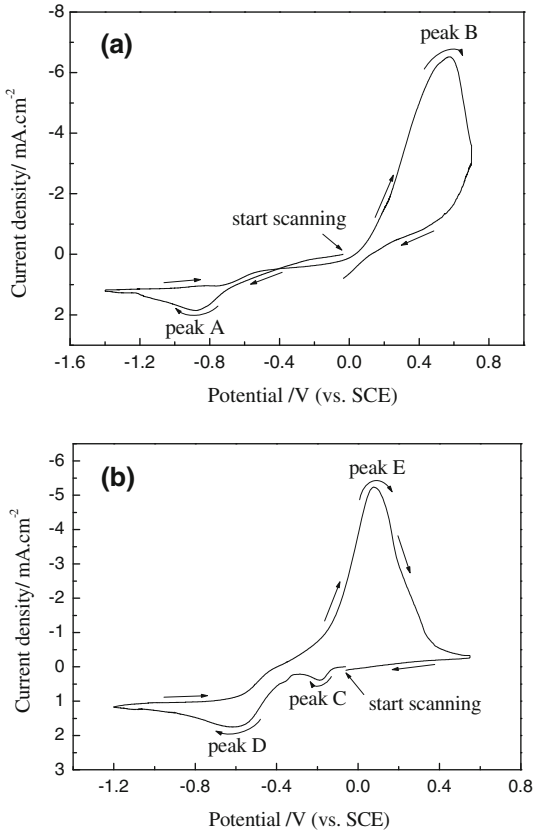

Fig. 1. Cyclic voltammograms of individual Te^{IV} and Sb^{III} solution systems containing (a) 20 mM $SbCl_3$ and (b) 20 mM $TeCl_4$, separately; scan rate 10 mV/s.

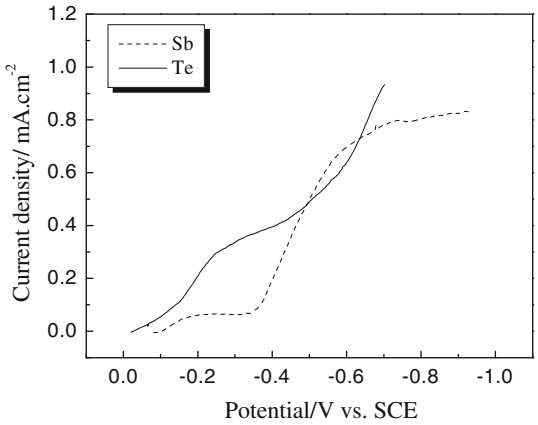

Fig. 2. Linear sweep voltammograms of Au electrode in unitary DMSO solutions containing 20 mM Te^{IV} (solid line) and 20 mM Sb^{III} (dashed line), respectively; scan rate 0.1 mV/s.

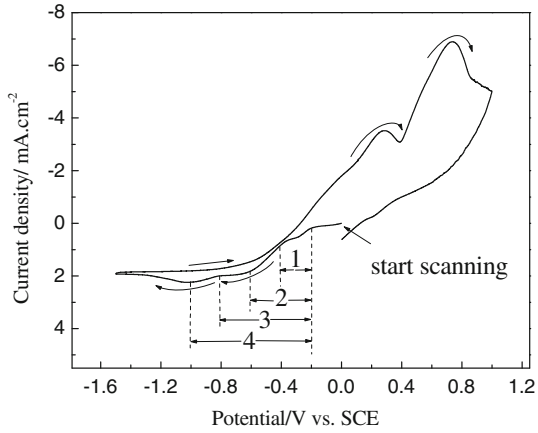

Fig. 3. Cyclic voltammogram of Au electrode in DMSO solution containing 20 mM Te^{IV} and 20 mM Sb^{III}; scan rate 10 mV/s.

Table II. Compositions of thermoelectric films potentiodynamically electrodeposited under different potential ranges from Sb-Te binary DMSO solution

	Atomic%		
Potential Range	**Sb**	**Te**	**Stoichiometry**
(1) −200 mV to −400 mV	23.23	76.77	$Sb_{1.16}Te_{3.84}$
(2) −200 mV to −600 mV	37.39	62.61	$Sb_{1.87}Te_{3.13}$
(3) −200 mV to −800 mV	55.26	44.74	$Sb_{2.76}Te_{2.24}$
(4) −200 mV to −1000 mV	71.72	28.28	$Sb_{3.59}Te_{1.41}$

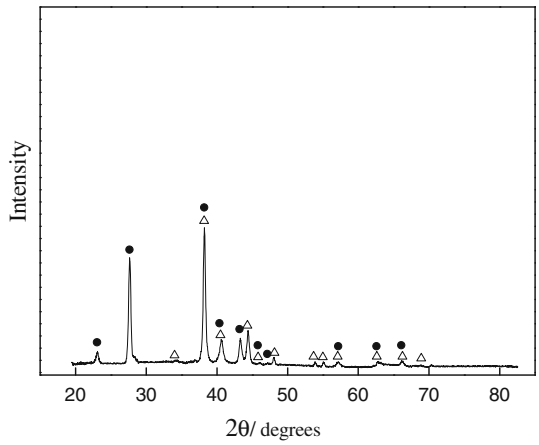

Fig. 4. XRD patterns of film potentiodynamically electrodeposited under the potential range of −200 mV to −600 mV from DMSO solution containing 20 mM Te^{IV} and 20 mM Sb^{III}, (Δ) Sb_2Te_3; (●) Te.

of Sb^{III} occurs through the following process: Sb^{III} around the cathode receives one electron firstly and is reduced to Sb(II) under low cathodic polarization potential, then Sb(II) receives two electrons and is further reduced to Sb^0. Comparing the two LSV results in Fig. 2, it can be found that reduction of Te^{IV} is comparatively easy, taking place at much lower polarization potential. This result is consistent with that from cyclic voltammetry.

Electrochemical Behaviors of Mixed Te^{IV} and Sb^{III} Solution System

The electrochemical behaviors of Te^{IV} + Sb^{III} mixtures were examined by cyclic voltammetry at

Table III. Morphology and thermoelectric performance of thermoelectric films potentiodynamically electrodeposited in different potential ranges from DMSO solution containing 20 mM $TeCl_4$, 20 mM $SbCl_3$, and 0.1 mM KNO_3

Potential Ranges	Morphology	After Annealing	
		ρ (Ω)	α (μV/K)
(1) −200 mV to −400 mV	Smooth and uniform	0.06	P 14
(2) −200 mV to −600 mV	Smooth and uniform	0.05	P 46
(3) −200 mV to −800 mV	Smooth and uniform	0.08	P 40
(4) −200 mV to −1000 mV	Smooth and uniform	0.06	P 39

10 mV/s in DMSO solution containing 20 mM Te^{IV} and 20 mM Sb^{III}, and corresponding results are shown in Fig. 3. Two wide reduction peaks can be observed in the cathodic branch of the CV curve, indicating that the reduction of Te^{IV} + Sb^{III} in DMSO solution to form Sb_xTe_y compound is completed in two steps, or that elemental Te^0 or Sb^0 in addition to Sb_xTe_y compound is formed during the cathodic scanning process and the two reduction peaks correspond to the formation of Sb_xTe_y compound and elemental Te^0 (or Sb^0), respectively.

Electrodeposition of Sb_xTe_y Thin Films in DMSO Solution

Sb_xTe_y thin films were potentiodynamically electrodeposited under different potential ranges in DMSO solution containing 20 mM Te^{IV} and 20 mM Sb^{III}. The corresponding positions of the four different potential ranges chosen to prepared the Sb_xTe_y thin films by potentiodynamic electrodeposition are labeled 1 to 4 in the CV curve in Fig. 3. The compositions of the electrodeposited films were analyzed using EDS, and the results are listed in Table II. It can be seen that all the films are composed of Sb and Te elements, indicating that Sb-Te binary thermoelectric material can be prepared from DMSO solution by potentiodynamic electrodeposition over a very wide potential range. With more negative potential, the atomic percentage of element Sb gradually increases while that of Te gradually decreases. $Sb_{1.87}Te_{3.13}$ thermoelectric film, which most closely approaches the stoichiometry of Sb_2Te_3, can be obtained in the potential range of −200 mV to −600 mV. The obtained film was also analyzed by XRD, and the result is shown in Fig. 4. It can be seen from the XRD pattern that the film electrodeposited in the potential range of −200 mV to −600 mV is composed of Sb_2Te_3 compound and element Te^0.

Table III presents the morphology and thermoelectric performance of the thermoelectric film potentiodynamically electrodeposited under different potential ranges from Sb-Te binary DMSO solution. It can be seen that all the deposited films possess uniform and smooth morphology. After annealing treatment at 200°C under N_2 protection for 4 h, all the films showed *p*-type semiconductor properties. It can also be found that the Seebeck coefficients of the films first increase then decrease gradually while their resistances remain almost unchanged as the potential range becomes more negative. The film potentiodynamically electrodeposited in the potential range of −200 mV to −600 mV possesses the highest Seebeck coefficient. This film is also the specimen whose stoichiometry most closely approaches that of the ideal compound Sb_2Te_3.

CONCLUSIONS

The electrochemical behavior of nonaqueous DMSO solutions of Te^{IV}, Sb^{III} was investigated by CV measurements. The results show that codeposition of Te^{IV}, Sb^{III} to form Sb_xTe_y thermoelectric material can be realized from DMSO solution. On this basis, Sb_xTe_y thermoelectric thin films were prepared by the potentiodynamic electrodeposition technique from nonaqueous DMSO solution, and the composition, morphology, and thermoelectric properties of the films were analyzed. The results show that Sb_xTe_y thermoelectric films prepared under different potential ranges all possessed smooth and uniform morphology. After annealing treatment at 200°C under N_2 protection for 4 h, all the deposited films showed *p*-type semiconductor properties. The $Sb_{1.87}Te_{3.13}$ thermoelectric film, which most closely approaches the stoichiometry of Sb_2Te_3 and possesses the highest Seebeck coefficient, can be obtained at potentials of −200 mV to −600 mV.

ACKNOWLEDGEMENTS

This work is co-supported by International Cooperation Project of Chinese Science and Technology Ministry (2009DFA62700), Doctorial Foundation Project of Chinese Education Ministry (200800560002), and the Key Technologies R&D Program of Tianjin (09ZCKFSF01200).

REFERENCES

1. B.Y. Yoo, C.-K. Huang, J.R. Lim, J. Herman, M.A. Ryan, J.-P. Fleurial, and N.V. Myung, *Electrochim. Acta* 50, 4371 (2005).
2. E.J. Menke, M.A. Brown, Q. Li, J.C. Hemminger, and R.M. Penner, *Langmuir* 22, 10564 (2006).
3. S. Li, M.S. Toprak, H.M.A. Soliman, J. Zhou, M. Muhammed, D. Platzek, and E. Müller, *Chem. Mater.* 18, 3627 (2006).
4. F.-H. Li and W. Wang, *J. Appl. Electrochem.* 40, 2005 (2010).
5. J. Li, B. Wang, F. Liu, J. Yang, J. Li, J. Liu, M. Jia, Y. Lai, and Y. Liu, *Electrochim. Acta* 56, 8597 (2011).

6. F. Xiao, C. Hangarter, B. Yoo, Y. Rheem, K.-H. Lee, and N.V. Myung, *Electrochim. Acta* 53, 8103 (2008).
7. F.-H. Li, Q.-H. Huang, and W. Wang, *Electrochim. Acta* 54, 3745 (2009).
8. J. Kuleshova, E. Koukharenko, X. Li, N. Frety, I.S. Nandhakumar, J. Tudor, S.P. Beeby, and N.M. White, *Langmuir* 26, 16980 (2010).
9. J.-H. Lim, M.Y. Park, D.C. Lim, B. Yoo, J.-H. Lee, N.V. Myung, and K.H. Lee, *J. Electron. Mater.* 40, 1321 (2011).
10. Y. Miyazaki and T. Kajitani, *J. Cryst. Growth* 229, 542 (2001).
11. Y. Qin, W. Chunfen, L. Shengcong, and C. Lidong, *Rare Metal Mater. Eng.* 36, 419 (2007).
12. H. Ebe, M. Ueda, and T. Ohtsuka, *Electrochim. Acta* 53, 100 (2007).
13. W.-J. Li, W.-L. Yu, and C.-Y. Yen, *Electrochim. Acta* 58, 510 (2011).
14. F.-H. Li, W. Wang, and J. Gao, *J. Electron. Mater.* 39, 1562 (2010).